Mitigating Capacity Fade by Constructing Highly-Ordered Mesoporous Al_2O_3/Polyacene Double-Shelled Architecture in Li-Rich Cathode Materials
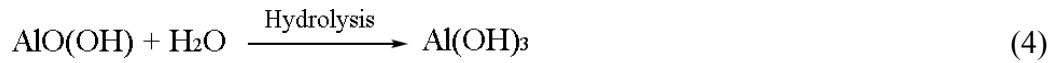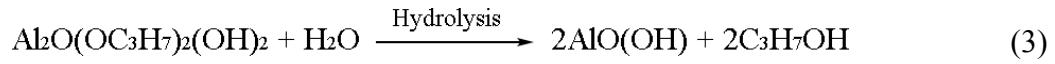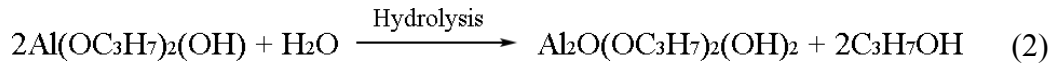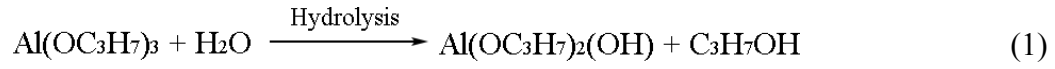
Ming Xu, Zhaoyong Chen[*], Huali Zhu, Xiaoyan Yan, Lingjun Li, Qunfang Zhao

School of Physics and Elctronic Science, Changsha University of Science and Technology, Changsha, 410004, Hunan Province, China.
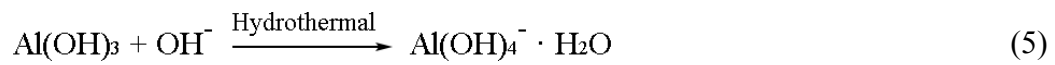
[*]Corresponding Author: Prof. Zhaoyong Chen, chenzhaoyongcioc@126.com

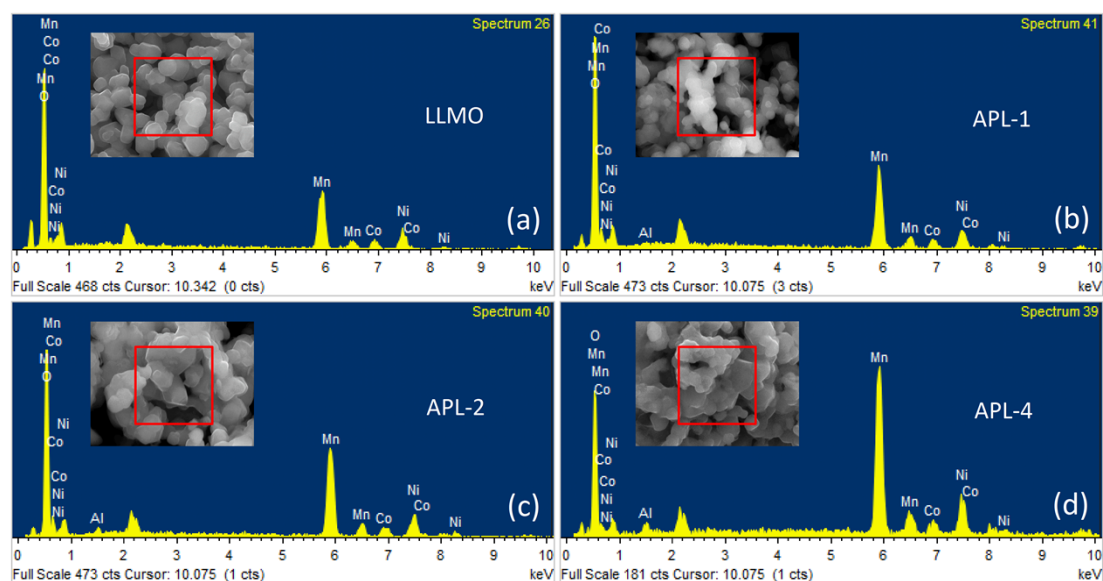**Chemical Mechanism of Hydrolysis of Aluminium Isopropoxide (AIP)**

The distilled water is added into the AIP solution and keep stirring at 80℃ for 4h, during which the Al(OH)$_3$ sol is formed. The reactions, such as hydrolysis of AIP and formation of Al$_2$O$_3$, are simplified as follows:

$$Al(OC_3H_7)_3 + H_2O \xrightarrow{\text{Hydrolysis}} Al(OC_3H_7)_2(OH) + C_3H_7OH \qquad (1)$$

$$2Al(OC_3H_7)_2(OH) + H_2O \xrightarrow{\text{Hydrolysis}} Al_2O(OC_3H_7)_2(OH)_2 + 2C_3H_7OH \qquad (2)$$

$$Al_2O(OC_3H_7)_2(OH)_2 + H_2O \xrightarrow{\text{Hydrolysis}} 2AlO(OH) + 2C_3H_7OH \qquad (3)$$

$$AlO(OH) + H_2O \xrightarrow{\text{Hydrolysis}} Al(OH)_3 \qquad (4)$$

Afterwards, the PL-5 powders are added into the Al(OH)$_3$ sol with constant stirring. The Al(OH)$_3$ sol might migrate on the surface of PL-5 powders to form a uniform coating layer, driven by thermodynamic forces to reduce the structure's total surface energy. Then the mixture is transferred into a Teflon-lined autoclave to capture Al(OH)$_3$, and a highly ordered mesoporous Al$_2$O$_3$ coating layer is formed after calcination at 500℃ for 4 h.

$$Al(OH)_3 + OH^- \xrightarrow{\text{Hydrothermal}} Al(OH)_4^- \cdot H_2O \qquad (5)$$

$$Al(OH)_4^- \cdot H_2O \xrightarrow{\text{Calcination at 500 ℃}} Al_2O_3 \qquad (6)$$
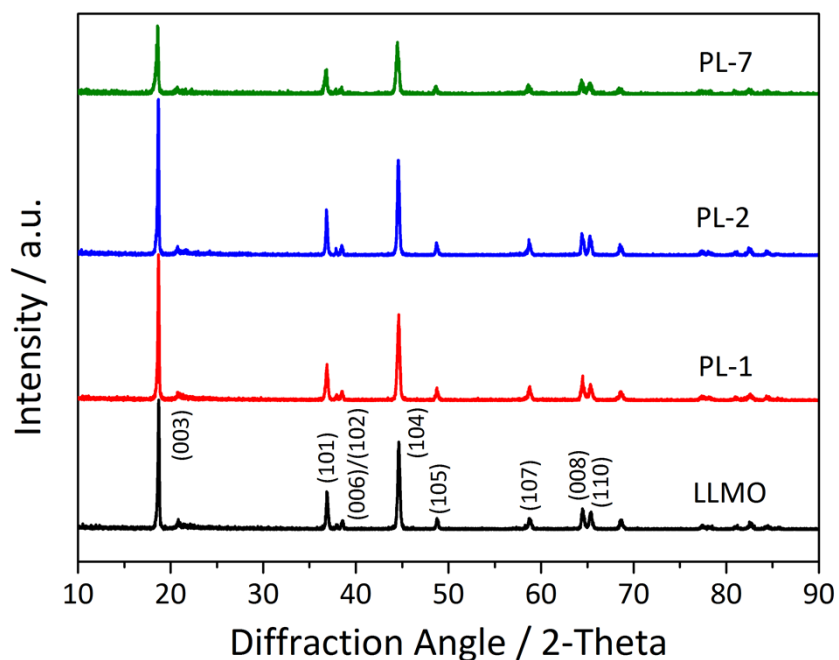
Figure S1

Energy-dispersive X-ray spectroscope (EDXS) of (a) LLMO, (b) APL-1, (c) APL-2, (d) APL-4 cathode materials based on the inset SEM images.

Table S1

| Elements	Samples (atomic ratio / %)			
	LLMO	APL-1	APL-2	APL-4
Ni	6.37	7.32	7.03	6.74
Co	2.10	3.17	3.14	3.65
Mn	16.17	16.80	16.92	17.11
Al	-	0.74	1.40	2.28

Atomic ratio of bare LLMO and double-shelled samples obtained from EDXS.

Figure S2

Calibrated XRD patterns of bare LLMO, PL-1, PL-2 and PL-7 samples are shown in Figure S2. All diffraction peaks can be indexed based on a layered structure with both rhombohedral symmetry (R-3m) and monoclinic structure (C/2m). The XRD patterns of PL-1 and PL-2 samples are consistent with that of bare LLMO sample, indicating that low PAS coating amount doesn't have any effect on the crystal strcuture of LLMO materials. However, as we can observe, the XRD pattern of PL-7 sample shows lower diffraction intensity due to the higher reducibility of 7 wt. % PAS amount.

Figure S3
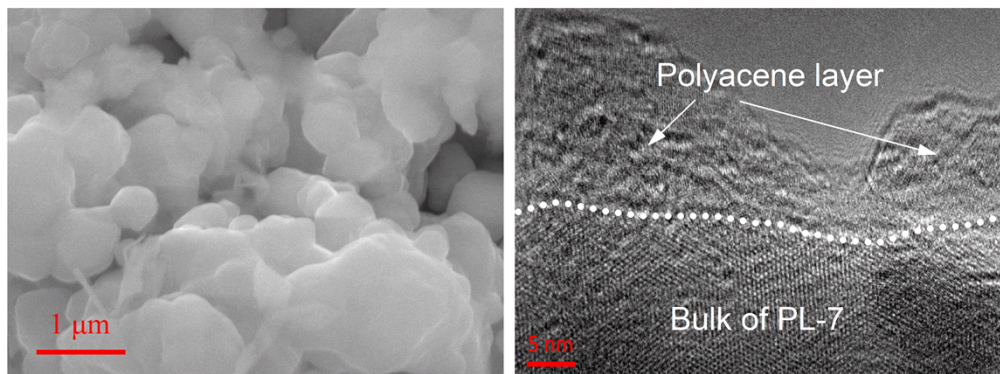
SEM and HRTEM images of PL-7 sample are shown in Figure S3. As shown in SEM image, the particles of PL-7 aggregated severely and the surface of particles is much more obscure due to 7 wt. % PAS coating. The HRTEM image of PL-7 sample shows the thick PAS layer which unhomogeneously distributed on the surface of PL-7 particles.

Figure S4
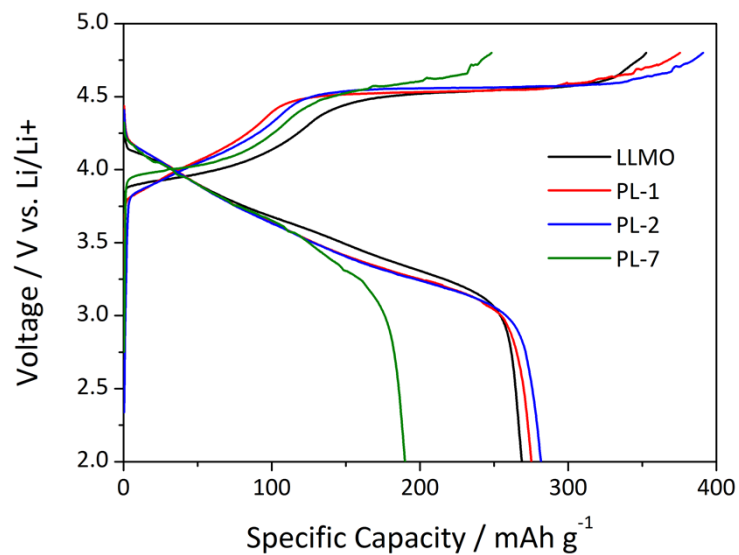
Initial voltage profiles of bare LLMO, PL-1, PL-2 and PL-7 samples between 2.0 and 4.8 V at 0.1 C (=20 mA g^{-1}). The bare LLMO material shows the initial discharge capacity of 269 mAh g^{-1}, while PL-1, PL-2 and PL-7 samples exhibit 275 mAh g^{-1}, 281 mAh g^{-1} and 187 mAh g^{-1} respectively. These resluts demonstrate that the 7 wt. % coating amount of PAS is not favourable for both crystal structure and electrochemical performance of LLMO materials.

Figure S5
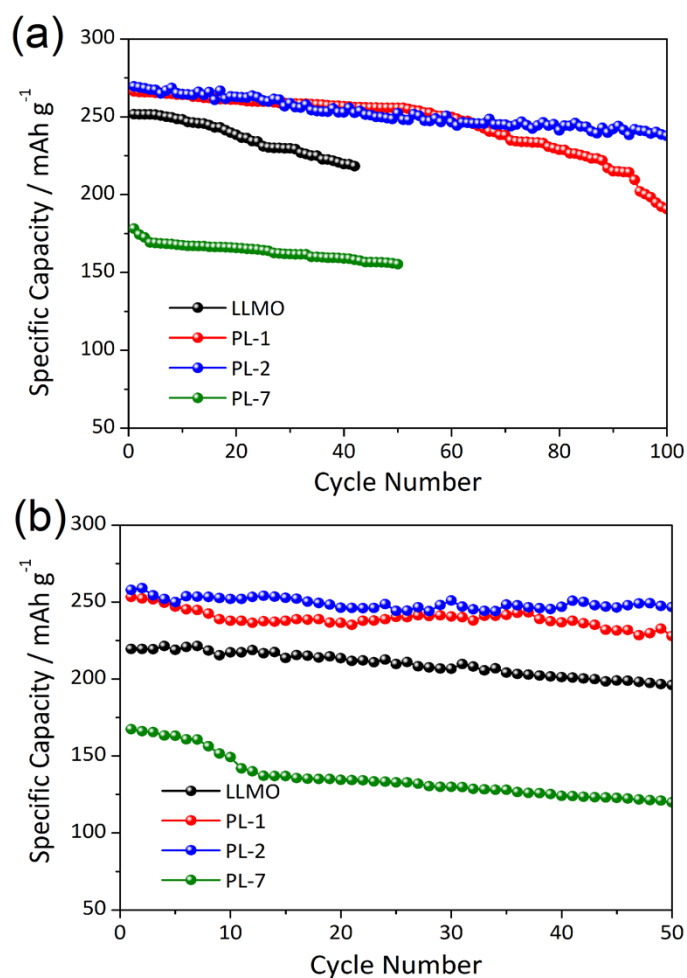
The variation of discharge capacity as a function of cycle number is performed to evaluate the capacity retention of the bare LLMO, PL-1, PL-2 and PL-7 samples: (a) at 0.2C; (b) at 1C. The capacity loss of LLMO is 15% even after 40th cycle; It is 29% and 10 % for PL-1 and PL-2 smaples respectively after 100th cycle at 0.2C rate between 2.0-4.8 V. It is noted that the PL-7 sample suffers 17% capacity loss after 50th cycle at 0.2C. The bare LLMO, PL-1, PL-2 and PL-7 suffered 15 %, 11%, 5% and 29 % capacity loss respectively after 50th cycle at 1C.